GEOTHERMICA

COntrol **SEIS**micity and **M**anage Induced earth**Q**uakes (**COSEISMIQ**)

Deliverable WP4

Deliverable WP4 (Month 18): Risk and Safety assessment calibrated for Icelandic conditions and extended to allow the distinction between natural and induced seismicity

Authors: ETH (Dr. M. Broccardo, Dr. A. Mignan, Dr. D. Karvounis, Dr. F. Grigoli, Dr. A.P. Rinaldi, Prof. S. Wiemer)

Publication Date: 08.12.2019

The GEOTHERMICA is supported by the European Union's HORIZON 2020 programme for research, technological development and demonstration under grant agreement No 731117

Deliverable WP4 (Month 18): Risk and Safety assessment calibrated for Icelandic conditions and extended to allow the distinction between natural and induced seismicity

Summary

Related to the *"Risk and Safety assessment calibrated for Icelandic conditions and extended to allow the distinction between natural and induced seismicity"*, we present the basis for a coherent hazard and risk management framework for fluid-induced seismicity in the Hengill region in Iceland. Specifically, we first discuss in detail the progress on both analytical and computational tools for an a-priori hazard and risk assessment and, second, we introduced a Bayesian updating scheme to integrate real-time monitoring with online hazard and risk updating. The proposed hazard computation is based on classical Probabilistic Seismic Hazard Analysis (PSHA) adapted for fluid-induced seismicity. Next, the risk computation is based on the convolution of hazard curves together with the vulnerability models tuned to the Icelandic built environment. The outputs of the framework are Individual Risk and Damage Risk, which are two metrics used for decision making in the Real-Time Induced Seismicity Controller (RISC) system. In the updating scheme, both the hazard output and the risk metrics are updated online based on real-time seismic monitoring. We tested the proposed framework for a synthetic case test, showing a potentially significant reduction of epistemic uncertainties that are currently present in the source modeling parameters. The document is structured as follow: In Section 1, we introduce the Hazard modulus together with its components (i.e., Source models, Magnitude Frequency distribution, GMPEs selection); In Section 2, we introduce the Risk modulus together with its components (i.e., vulnerability models, risk metrics), and Section 3 the updating scheme. At current time, no results are available for the classification of natural vs induced seismic events due to ambiguity to distinguish both sources.

1. Probabilistic induced seismic hazard framework

Probabilistic risk assessment is rapidly becoming the standard approach to manage and mitigate fluid-induced seismicity (Grigoli et al., 2017; Bommer et al., 2015; Broccardo et al. 2017a; Lee et al., 2019). The call for probabilistic approach and a risk-based approach are motivated by the stochastic nature of earthquakes, the significant uncertainties associated with the process of inducing seismicity, and the needs of regulators, insurances, and the public. This deliverable describes the general probabilistic hazard and risk assessment for the Hengill region in Iceland. In particular, in this section we focus on the PSHA analysis while Section 2 on the risk computation.

The essence of PSHA is the computation of the probability of exceeding a given intensity at a given distance d from the injection site, based on the number of events above a given minimum magnitude m_0, the frequency distribution of the magnitude (namely the truncated Guttenberg-Richter distribution), and an empirical ground shaking attenuation function. The latter can be an intensity prediction equation (IPE) based on felt intensity, or a ground motion prediction equation (GMPE) based on peak ground acceleration, spectral acceleration or peak ground velocity. Commonly, within this probabilistic framework, there are two main elements to be defined: (i) the probabilistic characterization of the seismogenic source model, and (ii) the ground motion characteristic model (describing the expected ground vibration given the occurrence of an earthquake). The first gives the

The GEOTHERMICA is supported by the European Union's HORIZON 2020 programme for research, technological development and demonstration under grant agreement No 731117

temporal and spatial forecast of the earthquake ruptures, while the second is characterized by Ground Motion Predictive Equations (GMPEs) to link the earthquake rupture with the expected ground shaking at the site of interest.

The outputs of PSHA are rate of exceedance or hazard curves (probability of exceedance for a given period of time) of a given ground shaking Intensity Measure type (IM). One single curve (for a given set of parameters) represents the aleatory (irreducible) variability. To include also the epistemic uncertainties, given the alternative models a logic tree structure with weighted branches (indicating the belief in a given model) is defined here. Figure 1 shows the proposed logic tree adopted after discussions between the authors of this deliverable for an a-priori risk analysis, which needs to be updated after local data and a local velocity model is available. The first level of the logic tree describes the (very large) epistemic uncertainty related to the selection of the seismogenic source parameters $[a_{fb}, b]$ of the model described later in the text while the second level on the uncertainty relates to the ground shaking model (i.e. choice of the appropriate GMPEs). The upper bound of the Gutenberg-Richter distribution is fixed, for Icelandic conditions, to $m_{sup} = 7$ (Kowsari et al., 2019).

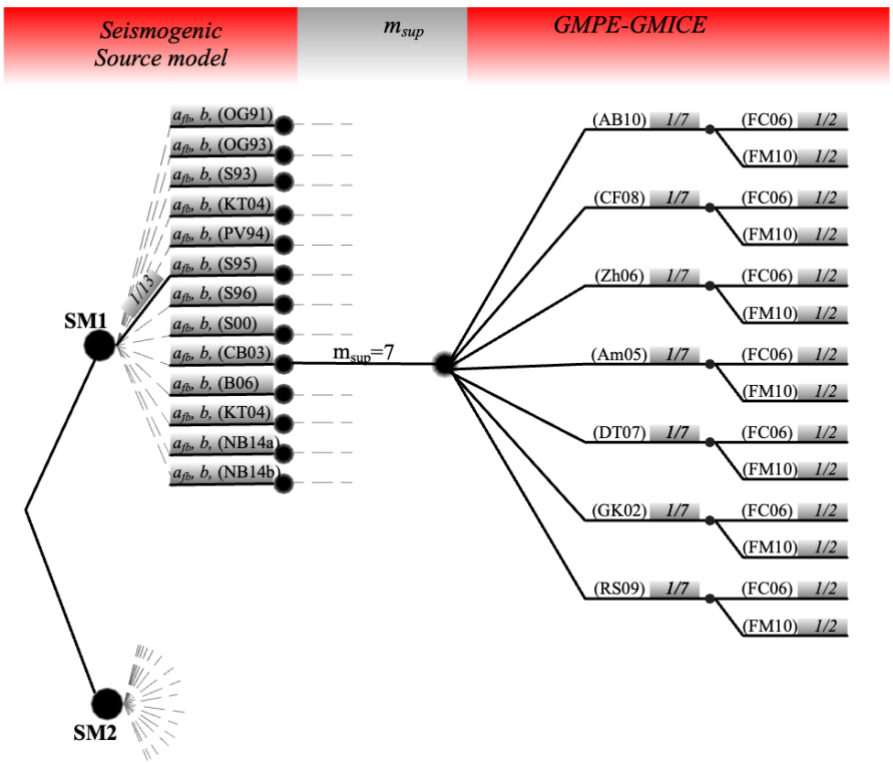

Figure 1 Logic tree for the PSHA analysis. Source (Broccardo et al., 2019) - See Table 2 for GMPE acronyms.

1.1 Seismogenic Source model, Existing analogues and empirical experience

In a first order type of analysis, we assume that induced seismicity nucleates and extends in the proximity of the injection points. Therefore, point sources located at the coordinates of the injection points are used as the unique source model for the study. This implicitly excludes any geometrical

The GEOTHERMICA is supported by the European Union's HORIZON 2020 programme for research, technological development and demonstration under grant agreement No 731117

uncertainty on the location of the hypocenter. The interaction between different wells has not been studied yet.

Forecasting the number of events occurring in a reservoir stimulation is difficult because in this area the stressing conditions and location of faults near the injection point are unknown. A pragmatic approach is to use empirical data from similar sites as a first-order proxy. In light of these deep uncertainties, we argue that simple models are preferable since they tend to be more robust, reducing the risk of overfitting. Moreover, simple models can more easily be updated with real-time data.
PSHA for natural seismicity is based on three parameters that describe the local activity rate, the size distribution, and the largest events size (Cornell, 1968). For induced seismicity, the models for hazard assessment likewise must also describe these three parameters.
We consider two simple models to analyze the uncertainty and to have a first order prior distribution of the underground response to injection:

I. *Model SM1* assumes the underground feedback is site-specific constant.
II. *Model SM2* simulates the fluid and overpressure propagation for the planned injection protocol based on one-dimensional diffusion and stochastically distributed seeds. This model is one-dimensional and the spatial interaction between different wells (or a more complex model, such as full 3D geomechanical models) has not been tested yet.

These two models capture to a first order the epistemic uncertainty in forecasting seismicity, since they express alternative approaches (the first purely statistic based, the second with embedded a physical diffusion process) to forecasting. We combine both models in the hazard computation with a weight of 50% each.

1.2 Model SM1

SM1 assumes that the "seismic underground feedback" per volume affected by significant pore-pressure change is a site-specific constant. This constant can vary by several orders of magnitudes between sites. Empirical evidence shows that the volume affected scales with the volume of fluid injected; this implies a relation between the expected number of earthquakes $E[N]$ and the volume injected V, which is written as

$$E[N(t); M > m] = \begin{cases} 10^{a_{fb}-bm}\dot{V}(t), t \leq T_{in} \\ 10^{a_{fb}-bm}\tau \exp\left(-\frac{t-T_{in}}{\tau}\right)\dot{V}(T_{in}), t > T_{in} \end{cases}, \quad (1)$$

where a_{fb} is the so-called underground feedback parameter (i.e., the overall activity for a given volume V), b is the b-value in a Gutenberg-Richter distribution, T_{in} is the injection duration, and τ is the mean relaxation time of a diffusive process (Mignan et al., 2017). Moreover, one can easily show that the expected total number of fluid-induced earthquakes is $E[N(\infty); M > m] = 10^{a_{fb}-bm}\left(V(T_{in}) + \tau\dot{V}(T_{in})\right)$. This relation is well known and accepted in the technical community as a first order model and sometimes also referred to as the Seismogenic Index model (e.g. Dinske and Shapiro, 2013; van der Elst et al., 2016; Mignan, 2016; Broccardo et al., 2017b). This model has been verified for a number of fluid injection experiments, in terms of flow rate Qstim (or ΔV) versus induced seismicity rate λ (Mignan et al., 2017). The model can also be redefined in term of rate function, i.e. $E[N(t); M > m] = \lambda(t; M > m)$ (Broccardo et al., 2017), which allows to define a Non-Homogenous Poisson Process (NHPP).

The GEOTHERMICA is supported by the European Union's HORIZON 2020 programme for research, technological development and demonstration under grant agreement No 731117

It is important to observe that this model only applies to the stimulation phase in which the fluids injected are not supposed to be back produced (i.e., negative flow rate). While the underground feedback parameters a_{fb} and b can be estimated during the stimulation (Mignan et al., 2017; Broccardo et al., 2017b), a priori knowledge on those parameters is very limited and the range of possible values is very wide. In Table 1, we list parameter estimates for different sites, which will be used as input for the a-priori risk study. Uncertainties are likely to collapse once seismic data is obtained by monitoring during the stimulation.

Table 1 Underground seismic feedback to deep fluid injection.

Site (country*, year)	a_{fb}†	b	$\lambda_{M\geq 2}$	References
Ogachi OG91 (JP, 1991)	-2.6	0.7	4.3800	Dinske and Shapiro (2013)
Ogachi (JP, 1993)	-3.2	0.8	0.6942	Dinske and Shapiro (2013)
Soultz (FR, 1993)	-2.0	1.4	0.6942	Dinske and Shapiro (2013)
KTB (DE, 1994)	-1.4	0.9	27.6359	Mignan et al. (2017)
Paradox Valley (US, 1994)	-2.4	1.1	1.1002	Mignan et al. (2017)
Soultz (FR, 1995)	-3.8	2.2	0.0003	Dinske and Shapiro (2013)
Soultz (FR, 1996)	-3.1	1.8	0.0087	Dinske and Shapiro (2013)
Soultz (FR, 2000)	-0.5	1.1	87.3925	Dinske and Shapiro (2013)
Cooper Basin (AU, 2003)	-0.9	0.8	138.5078	Dinske and Shapiro (2013)
Basel (CH, 2006)	0.1	1.6	34.7916	Mignan et al. (2017)
KTB (DE, 2004-5)	-4.2	1.1	0.0174	Dinske and Shapiro (2013)
Newberry (US, 2014a)	-2.8	0.8	1.7437	Mignan et al. (2017)
Newberry (US, 2014b)	-1.6	1.0	11.0021	Mignan et al. (2017)

* ISO code; † referred to as seismogenic index in Dinske and Shapiro (2013).

1.3 Model SM2

Model S2 introduced a first-order physical process into the forecasting. This is achieved by modeling pressure diffusion through a fractured media containing randomly distributed earthquake faults (so called "seeds"). The pressure propagation can be adopted based on the reservoir properties, as much as they are known. The density of these seeds, and the size distribution, are then free parameters that again are a priori unknown, site specific parameters. These models are commonly referred to as "hybrid" models (Gischig and Wiemer, 2013; Goertz-Allman and Wiemer, 2013) as they combine deterministic and stochastic modelling.

In this implementation, induced seismicity scenarios are stochastically modelled by sampling random hydro-shearing scenarios based on the existing field knowledge. Then, deterministic modeling of flow for a calibrated reservoir model returns which of these scenarios can indeed be realized because of the planned injection. Here, the adaptive Hierarchical Fracture Representation (a-HFR) is employed both for modeling flow in a fracture network with dynamically changing permeability (Karvounis and Jenny, 2016) and for simulating the source times of randomly pre-sampled scenarios of hydro-shearing events at certain hypocenter (Karvounis et al., 2014). Initially, a-HFR simulates the diffusion of overpressure for the planned injection inside a geological model with the observed transmissibility and compressibility. Whenever the simulated overpressure satisfies the failure condition at one of the randomly sampled scenarios, then the permeability increases at the slipped surface, affects the evolution of overpressure thereafter, and the scenario is considered by the synthetic catalogue of induced seismicity. This hybrid model is chosen here, as it can integrate several of the field observations, returns forecasts both of the spatial distribution of seismicity and of its focal planes, and can forecast reservoir properties like the

The GEOTHERMICA is supported by the European Union's HORIZON 2020 programme for research, technological development and demonstration under grant agreement No 731117

expected well's injectivity at the end of the injection.

Minimum required inputs to this hybrid model are the initial hydraulic properties, the planned activity, and some knowledge of the stress conditions around the considered well and of the orientations of pre-existing fractures. The resulting seismicity rates can be converted into static equivalents rates (like for SM1) and compared with SM1. Specifically, Figure 2 shows the results together with case of synthetic catalogue with predefined parameter matching Icelandic conditions. The same comparison can and should be applied for more sophisticated 3D geomechanical models (under development in WP3).

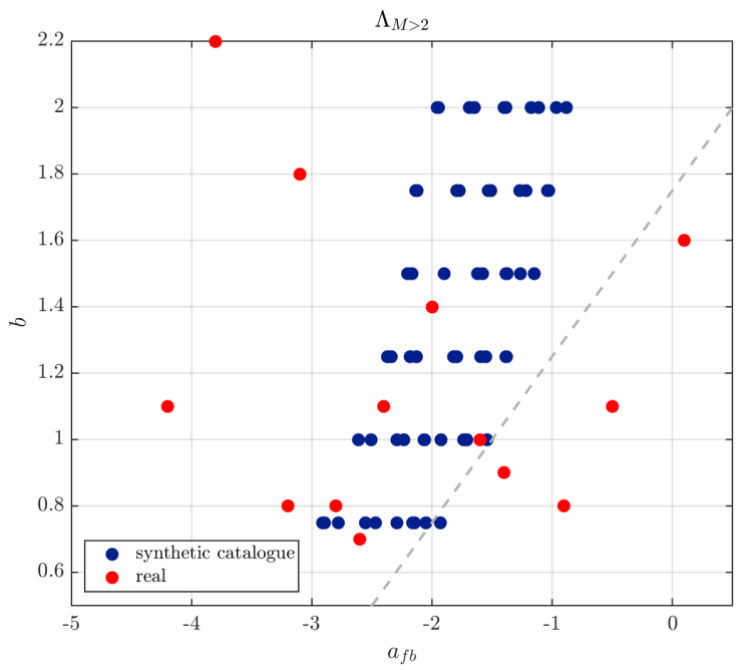

Figure 2 Distribution of a_{fb}- b values for the synthetic catalogue together with the dataset of Table 1. The dashed line represents the upper limit of no expected seismicity $M > 2$. Details can be found in Broccardo et al. 2019.

1.4 Ground Motion Prediction Equations

The relationship between the site source characteristics and ground shaking intensity measures, IMTs, is given by 7 GMPEs. The selection is based on the work of Kowsari et al. (2019), which they recalibrate existing GMPEs models used in SHARE (2009-2013) and other projects to the Icelandic strong motion data set. The recalibration dataset is based on six strike-slip events in the South Iceland Seismic Zone (SISZ), with a range of magnitudes between $M_w \in [5, 6.5]$, and distance $R \in [0,80]$ km. The intensity measures are reported in Table 2, and the value of the functional form and the coefficients can be retrieved directly from Kowsari et al. (2019). Observe that from the original list we replaced the proposed GMPE of Lin and Lee (2008) for North Taiwan with the local GMPE (RS09), Rupakhety and Sigjörnsson (2009), which is consistent with the strike-slip nature of Icelandic earthquakes. The recalibration has been performed only for the peak ground acceleration (PGA); therefore, in the following, we assume only this measure. The selected site-to-source distance is the Joyner-Boore metric (R_{JB}) (i.e., the closest horizontal distance to the vertical surface projection of the fault). When the distance metric of the

The GEOTHERMICA is supported by the European Union's HORIZON 2020 programme for research, technological development and demonstration under grant agreement No 731117

original GMPE is different from R_{JB}, the same transformations proposed in Rupakhety and Sigjörnsson (2009) are applied. Figure 3 shows the Trellis Plots for the selected GMPEs models.

Table 2 Selected list of GMPEs

GMPE name	Location	Reference
1-AB10	Europe & Middle East	Akkar Bommer (2010)
2-CF08	Worldwide	Cauzzi Faccioli (2008)
3-Zh06	Japan	Zhao *et al.* (2006)
4-Am05	Europe and Middle East	Ambraseys et al. (2005)
5-DT07	Greece	Danciu and Tselentis (2007)
6-GK02	Turkey	Gülkan and Kalkan (2002)
7-RS09	Iceland, Europe and MiddleEast	Rupakhety and Sigjörnsson (2009)

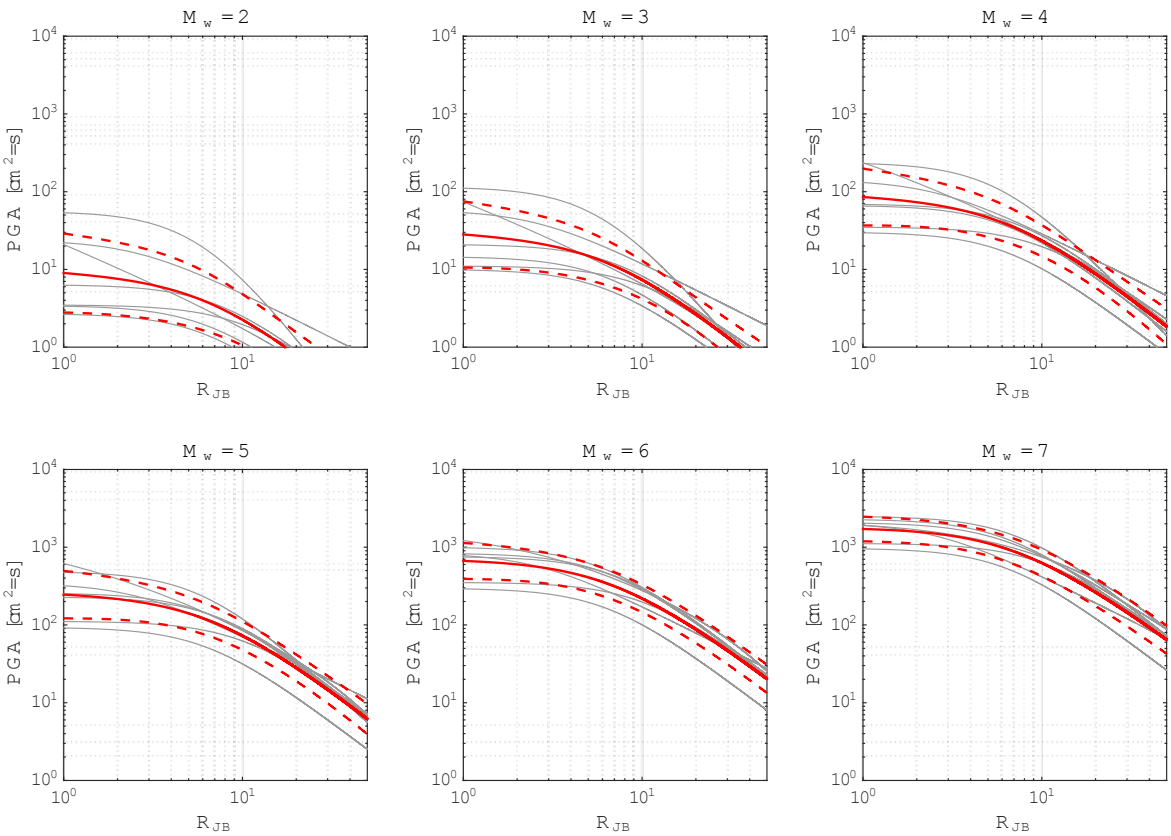

Figure 3. Trellis Plots for the selected GMPEs models. Following the same representation of Rupakhety and Sigjörnsson (2009), solid red lines are the epistemic mean and the dash lines the epistemic mean plus minus the epistemic standard deviation.

We then convert the PGA into the European Macroseismic Scale (EMS98, Grünthal, 1998). The advantage of EMS98 over physical based intensity measure, in this phase, lies in the easier interpretability of this scale, which is based merely on shaking indicators expressed in terms of damage and nuisance to the population. Based on these considerations, the selected GMPEs are converted into expected intensity by using Ground Motion to Intensity Conversion Equations (GMICE) for small-medium intensities. The GMICE used in this work are introduced by Faccioli and Cauzzi (2006) and Faenza and Michelini (2010). The aleatory variability is then combined into a GMPE-GMICE model with σ_{TOT}

The GEOTHERMICA is supported by the European Union's HORIZON 2020 programme for research, technological development and demonstration under grant agreement No 731117

defined as $\sigma_{TOT} = \sqrt{(\sigma_{GMPE}^2)a^2 + \sigma_{GMICE}^2}$, and values of mean μ, σ_{GMPE}, σ_{GMICE}, and a reported in Table 3. Figure 4 shows the GMICE epistemic range as function of distance and M_w.

Table 3. GMICE parameter list

	$\mu_{IM}(PGA)$	σ_{GMICE}		σ_{GMPE}	a	σ_{TOT}
Faccioli and Cauzzi (2006) Units: [m/s]	$1.96\log_{10}(PGA)+6.54$	0.89	1-AB10	0.175	1.96	0.954
			2-CF08	0.176	1.96	0.955
			3-Zh06	0.391	1.96/ln(10)	0.950
			4-Am05	0.175	1.96	0.954
			5-DT07	0.177	1.96	0.955
			6-GK02	0.403	1.96/ln(10)	0.954
			7-RS09	0.287	1.96	1.053
Faenza and Michelini (2010) Units: [cm/s]	$2.58\log_{10}(PGA)+1.68$	0.35	1-AB10	0.175	2.58	0.571
			2-CF08	0.176	2.58	0.573
			3-Zh06	0.391	2.58/ln(10)	0.560
			4-Am05	0.175	2.58	0.571
			5-DT07	0.177	2.58	0.575
			6-GK02	0.403	2.58/ln(10)	0.571
			7-RS09	0.287	2.58	0.819

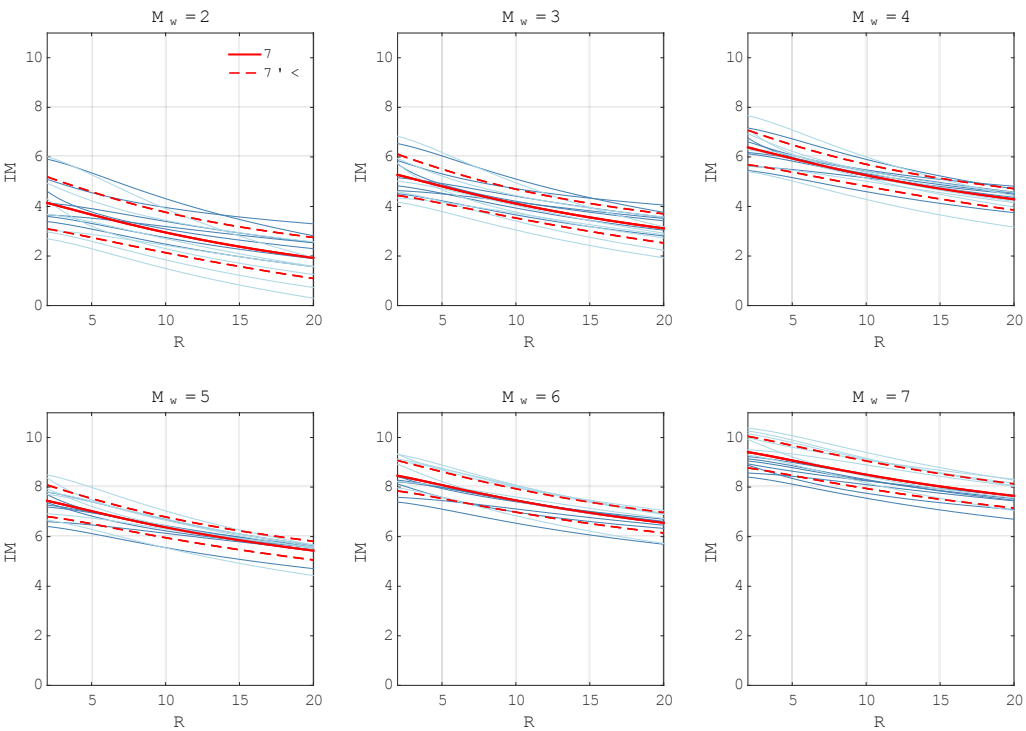

Figure 4 GMICE model. Solid red lines are the epistemic mean and the dash lines the epistemic mean plus minus the epistemic standard deviation.

The GEOTHERMICA is supported by the European Union's HORIZON 2020 programme for research, technological development and demonstration under grant agreement No 731117

1.5 Scenario Based intensity

Once the logic tree is completely defined, the hazard computation is given by classical convolution of all source of uncertainties for each branch. Given the large epistemic uncertainty governing the parameter a_{fb} and b of the seimogenic source model, we first compute the conditional probability distribution of PGA and IM: i.e., $P(PGA > pga|M = m, r) = \bar{\Phi}_{2\sigma}[(ln\, pga - \mu_{pga}(m,r))/\sigma_{GMPE}]$, $P(IM > im|M = m, r) = \bar{\Phi}_{2\sigma}[(ln\, im - \mu_{im}(m,r))/\sigma_{tot}]$, where $\bar{\Phi}_{2\sigma}[\cdot]$ is the CDF of the truncated standard normal distribution. The truncation is performed at $2\sigma_{TOT}$. Figure 5 and 6 show the collection of the epistemic PGA and IM medians for different magnitude events, from a given injection point for an average type of Icelandic Geothermal location.

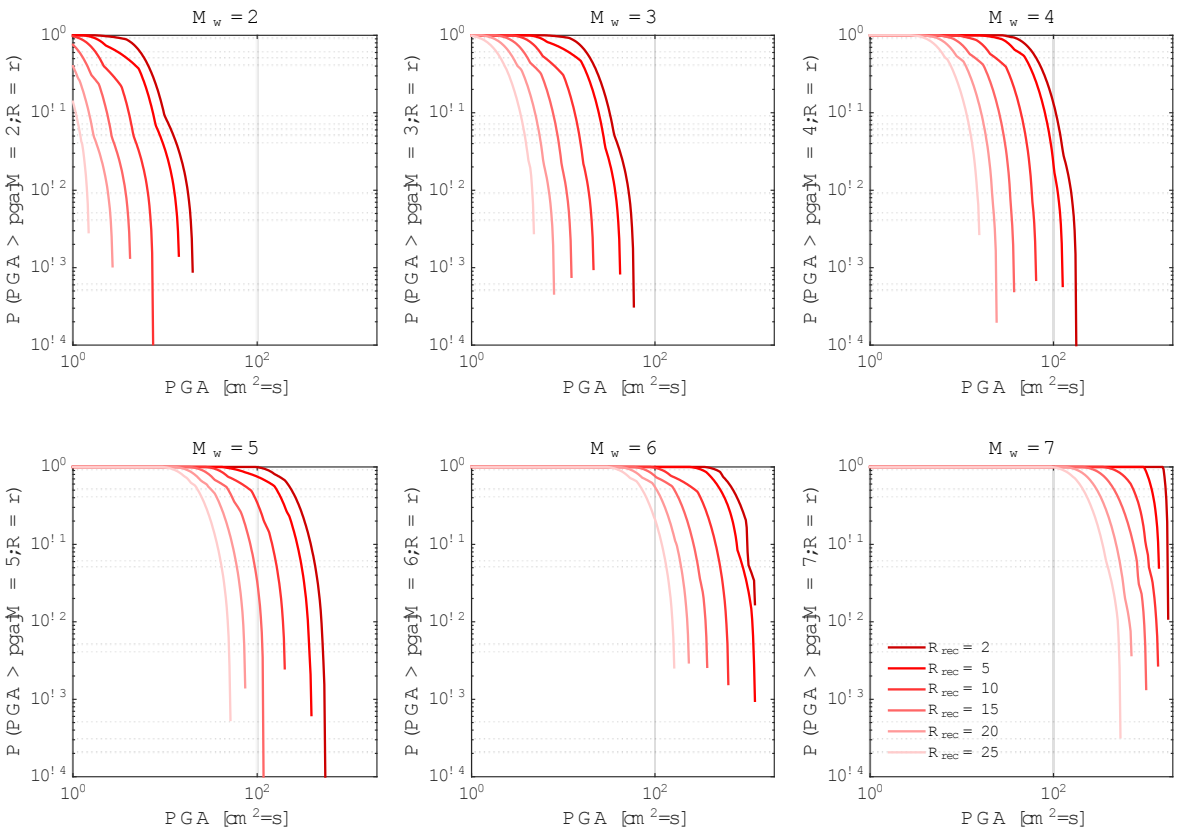

Figure 5 Collection of epistemic medians of $P(PGA > pga|M = m, R = r)$ for different magnitude and and site to source distances

The GEOTHERMICA is supported by the European Union's HORIZON 2020 programme for research, technological development and demonstration under grant agreement No 731117

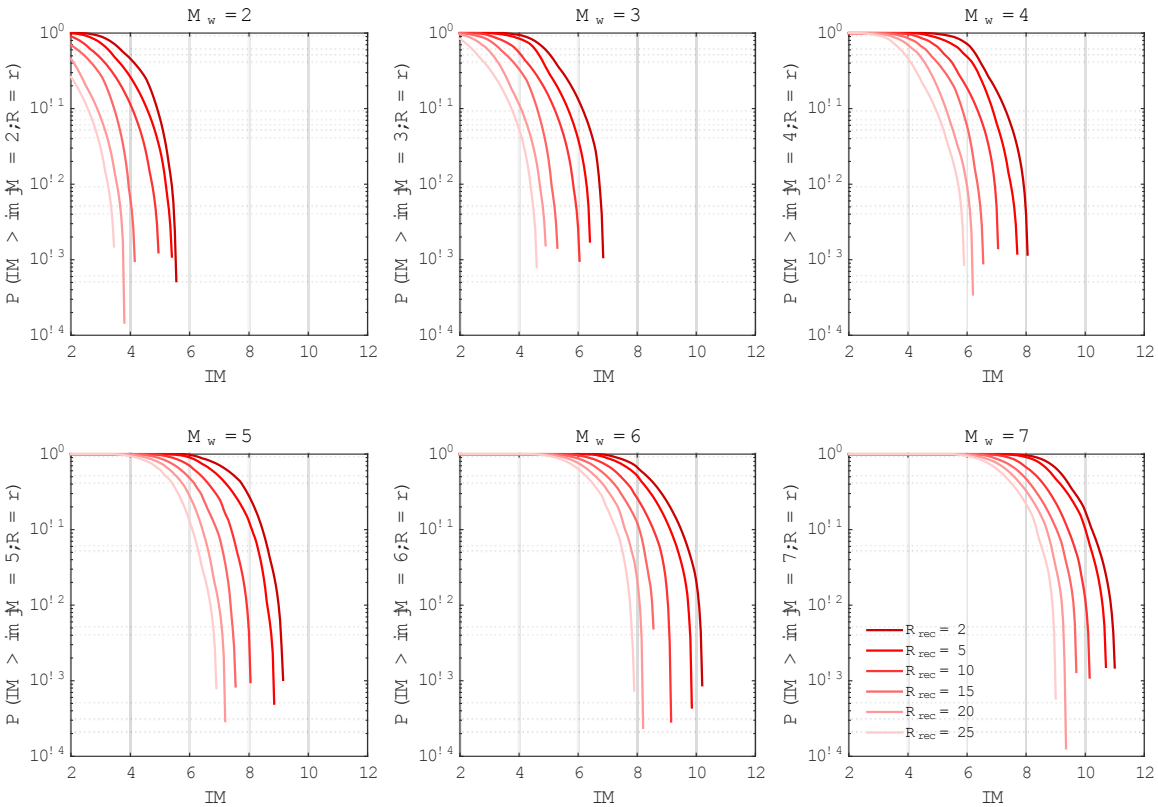

Figure 6 Collection of epistemic medians of $P(IM > im|M = m, R = r)$ for different magnitude and site to source distances

1.6 Probabilistic hazard computation

The hazard integral is condensed to the marginalization of the random variable magnitude, M, and the conditional random variable $IM|M = m$, since the site-to-source distance is fixed by the source point. For a given site, then the rate of exceedance is simply reduced to $\Lambda(im; T, b) = -\int_m P(IM > im|M = m, r)\, d\Lambda_{M>2}(m; T, b)$, where $F(m)$ is the Gutenberg-Richter above magnitude 2. The probability of exceedance of an intensity, $IM = im$, for a given time period, $t = 1$, (which corresponds to the total duration of the project given the normalization previously introduced), is given by the Poisson distribution as $P(IM > im, t = T) = 1 - \exp\big(-\Lambda(im; T, b)\big)$. However, $\Lambda_{M>2}(T)$ is not known a priori (neither an uncertainty quantification based on local condition can be carried out a-priori), therefore the risk is computed for each of the a_{fb} and b pairs of Table 1. Figure 7 and 8 show the PSHA outputs. In red are reported the real data and in blue the model SM2. No other 3D geomechanical outputs are available at the time of this deliverable. These curves confirm the state of deep uncertainty. In fact, for a given probability of exceedance of 10^{-4} and distance 2-5 km from the injection point, the macroseismic intensity range between the 10% and 90% percentile is circa $IM \in [6, 11]$. This corroborates the need for a robust real time updating.

The GEOTHERMICA is supported by the European Union's HORIZON 2020 programme for research, technological development and demonstration under grant agreement No 731117

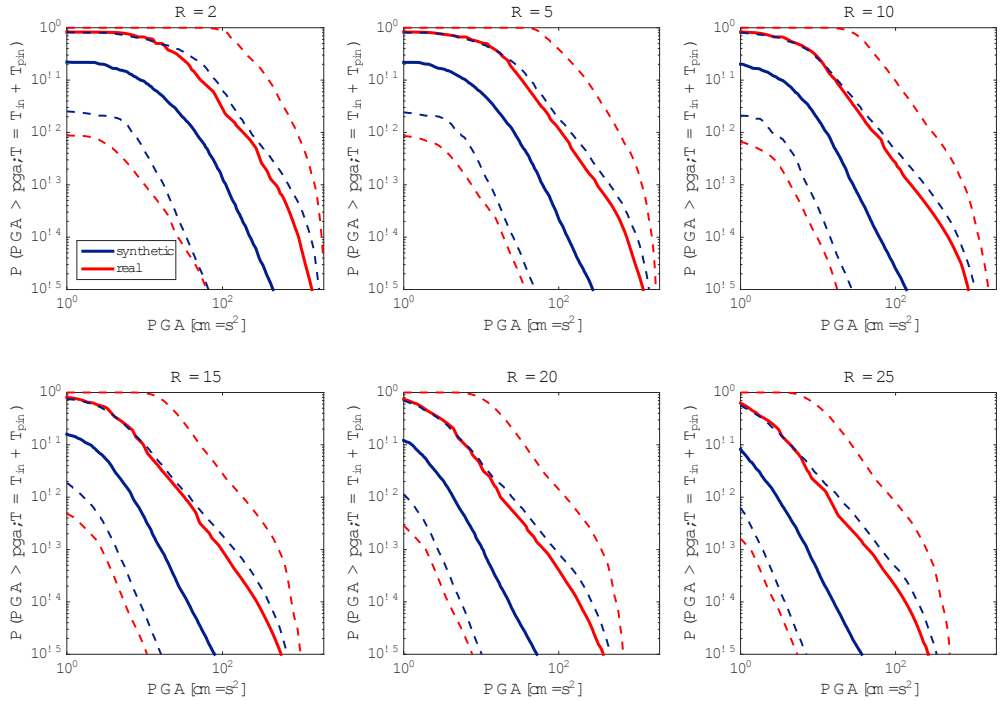

Figure 7 PSHA analysis comparison between source model SM1 (Table 1) and SM2 (synthetic catalogue). Solid lines: medians; dashed lines 10% and 90% quantiles. Intensity measure PGA.

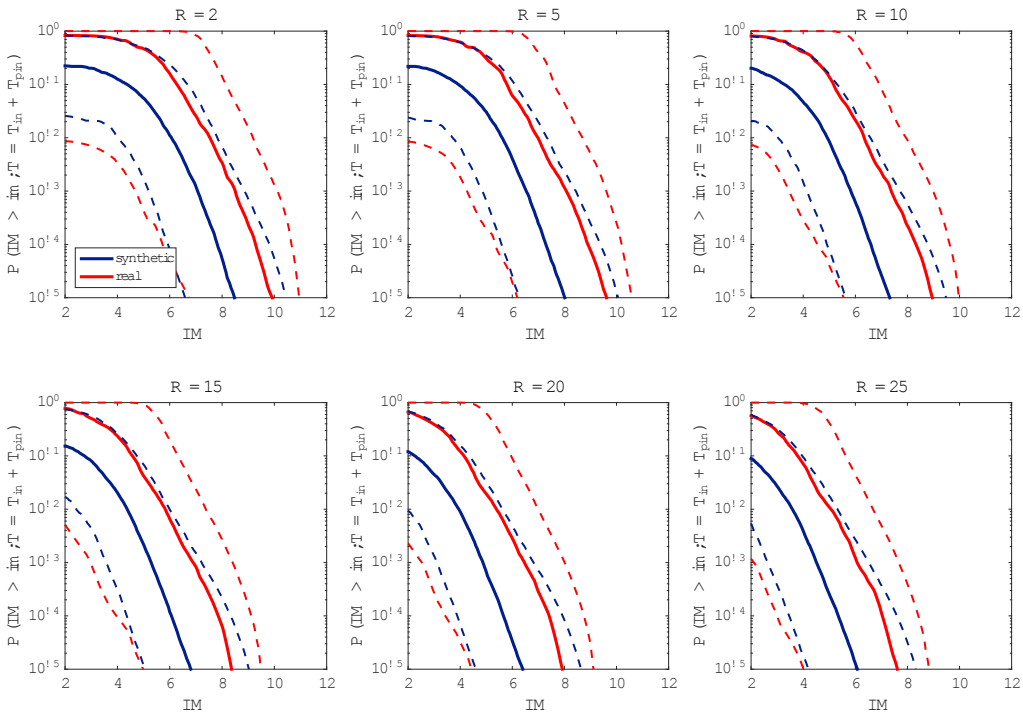

Figure 8 PSHA analysis comparison between source model SM1 (Table 1) and SM2 (synthetic catalogue). Solid lines: medians; dashed lines 10% and 90% quantiles. Intensity measure $EMS98$.

The GEOTHERMICA is supported by the European Union's HORIZON 2020 programme for research, technological development and demonstration under grant agreement No 731117

2. Probabilistic risk computation framework

In COSEISMIQ the risk analysis has limited impact due to low population density and limited building fragility. However, it is this special condition that makes the entire area and ideal site to test and validate COSEISMIQ tools. Therefore in the following we propagate the hazard analysis into the risk domain for a virtual Icelandic type of building. Seismic risk is computed by convolving a vulnerability model for the relevant building typologies with the exposure model. We define two risk measures: Individual Risk (IR) and Damage Risk (DR). For the fragility-vulnerability model we shall base our analysis on local functions. However, at the present time there exist only local fragility functions for low damage. The reference paper for such models is given by Bessason and Bjarnason (2015). Given that, we use the macroseismic intensity approach for IR (Lagomarsino and Giovinazzi, 2006), while using the local fragility function for DR.

2.1 Individual Risk

The IR is computed with vulnerability models that follow the macroseismic approach for damage assessment (Lagomarsino and Giovinazzi, 2006) and modified in Mignan et al., (2015) for the induced seismicity case. In this approach, the vulnerability is not defined based on detailed mechanical models; therefore, it is implicitly assumed that macroseismic and mechanical approaches produce compatible levels of damage. The macroseismic model defines the mean damage grade, $\mu_D(im)$, as function of a vulnerability index V, a ductility index, Q, and a reduction factor α introduced in Mignan et al. (2015) to recalibrate low damage states to the damage observed in the Basel 2006 sequence. The vulnerability index depends on the building class and construction specifics, and it includes following Lagomarsino and Giovinazzi (2006) probable ranges $V - V +$, as well as less probable ranges $V - -V + +$. Following the Icelandic exposure described in Bessason and Bjarnason (2016), we select three building typologies: Concrete, Wood and Masonry as a surrogate for Pumice buildings. Moreover, Bessason and Bjarnason (2016) observed that (in average) the Icelandic buildings are stronger and more reliable than the ones based on Euro-Mediterranean Region. Based on these considerations, we select V_0 as vulnerability index for Concrete and Wood, and V^- for masonry. The choice of V^- for masonry is given by the observation that the fragility of this building is close to old (before the 1980s) Icelandic reinforced concrete building. Moreover, there is no detailed information on the ductility index for the different class of building, therefore we use $Q = 2.3$, which is the value for masonry structures and reinforced concrete structure with no seismic details. The first analysis consists in IR scenarios for different magnitudes, locations and building typologies. The scenarios are derived by using the mean of the GMICE and converted into IR by using the vulnerability model and the conditional probability of fatalities for a given damage grade. Figure 9 shows the IR scenario-based calculations.

The GEOTHERMICA is supported by the European Union's HORIZON 2020 programme for research, technological development and demonstration under grant agreement No 731117

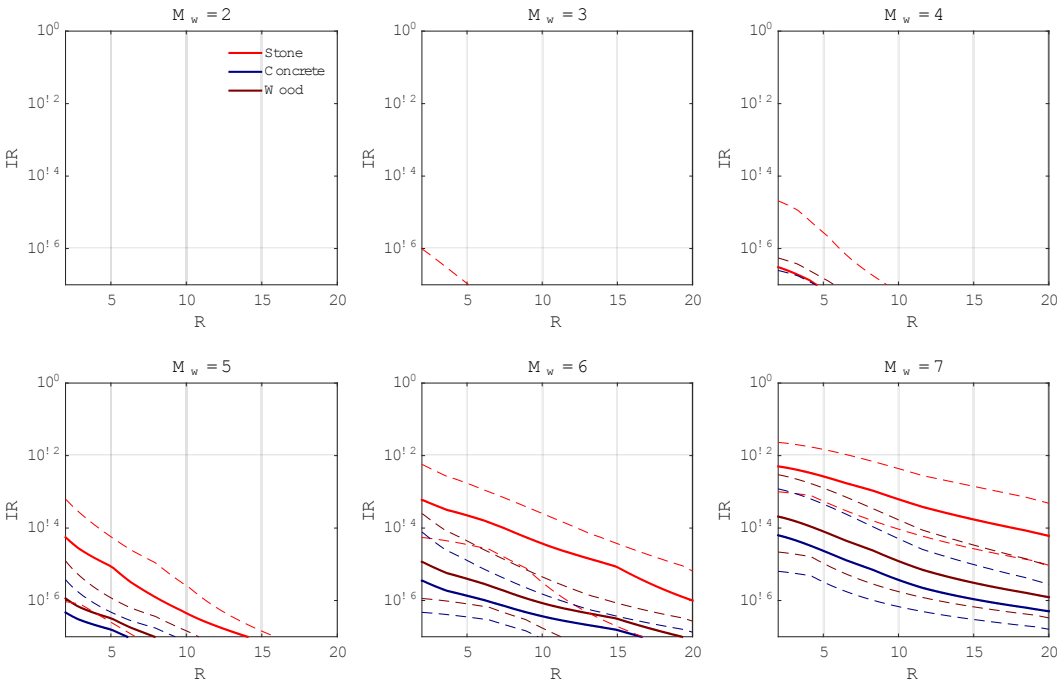

Figure 9. Individual Risk for different magnitude, distance and typology of buildings.

The second type of computation consist in the marginal IR considering all the $[a_{fb}, b]$ couples in a given location (i.e., different distances), for the total duration of the project. The results are shown in Figure 10 for each building class. Median and quantiles are computed considering a 50% weight for the SM1 model and 50% weight for SM2 model for the selected set of parameters.

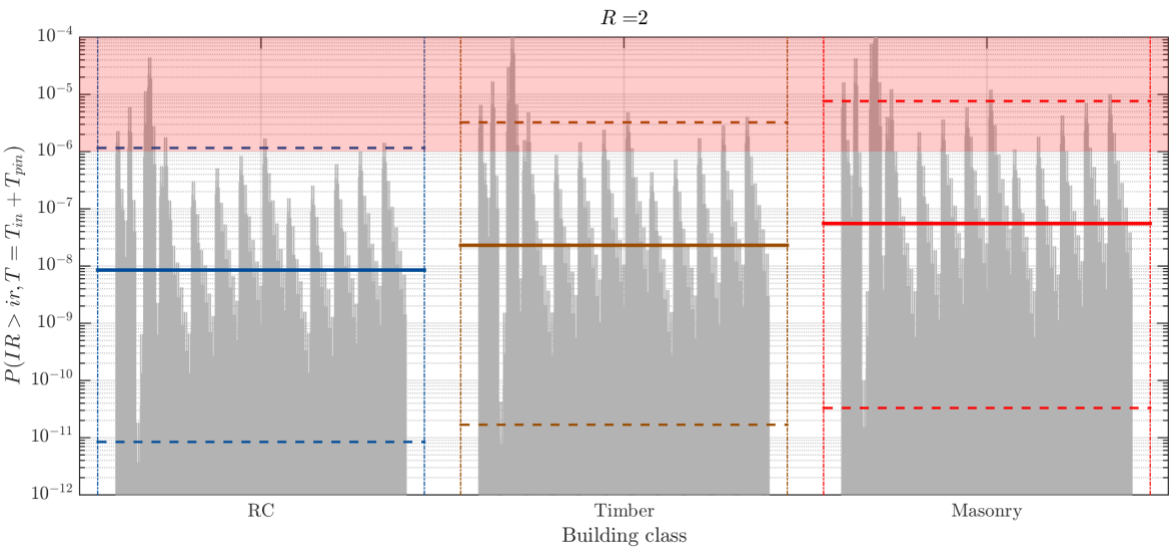

Figure 10 Marginal IR for 2 km distances based on the final model (combined SM1 and SM2) for a reasonable stimulation fluid volume to create a reservoir. The solid horizontal lines represent the weighted median values of the vertical gray lines. The dashed horizontal lines represent the 10 and 90% epistemic quantiles.

The GEOTHERMICA is supported by the European Union's HORIZON 2020 programme for research, technological development and demonstration under grant agreement No 731117

2.2 Damage Risk

For DR, we promote the use of the local fragility model developed by Bessason and Bjarnason (2015). Three major categories of buildings characterize the Icelandic exposure model: reinforced concrete, timber and hollow pumice block. Within these categories, Bessason and Bjarnason (2015) define the following subcategories:

I. *Low-rise reinforce concrete*

RC-b80: Reinforced concrete structure designed before seismic code regulations (before 1980).

RC-a80: Reinforced concrete structure designed after seismic code regulations (after 1980).

II. *Low-rise timber structures*

T-b80: Timber structure designed before designed before seismic code regulations

T-a80: Timber structure designed after designed before seismic code regulations

III. *Hollow pumice blocks* (**HP**)

Fragility functions are provided for all these categories only for small damages (which makes not possible the use for IR). Figure 11 shows the damage scenario for a magnitude 3 and 4, which represent the scenario limit for observing $DR \leq 10^{-2}$ on a virtual Icelandic building. Then, we compute the marginal DR considering all the $[a_{fb}, b]$ couples (for both the source model SM1, with weight 50%, and SM2 with weight 50%) in a given location. The results are shown in Figure 12 for each class of buildings.

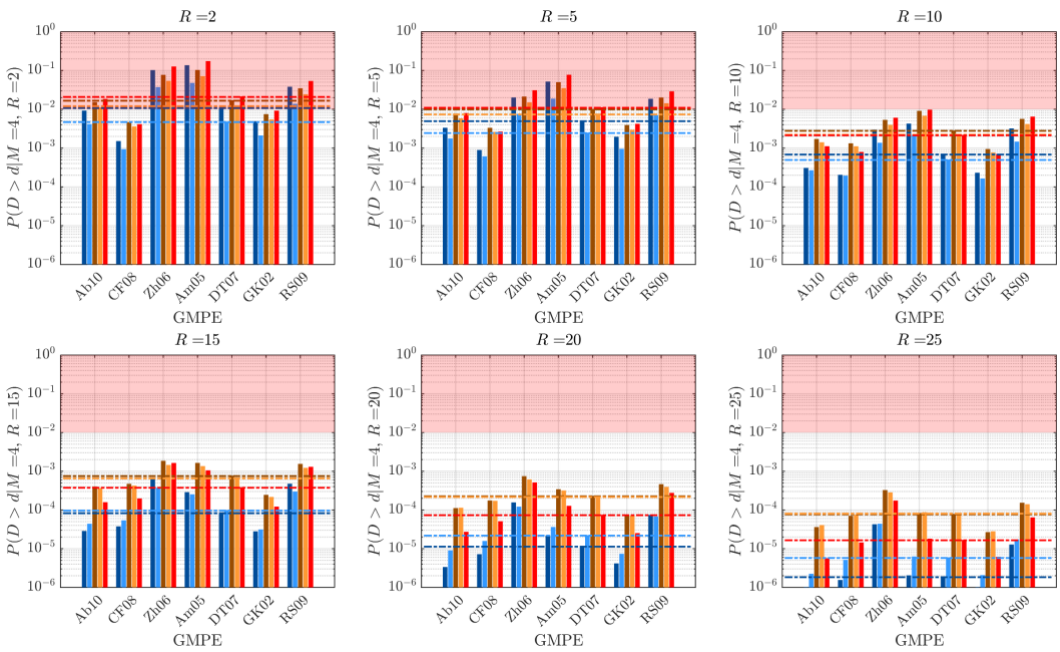

Figure 11. Scenario-based Damage Risk for magnitude 3. Different colours represent different building class: dark blue RC-b80, light blue RC-a80, dark brown T-b80, orange T-a80, and red HP.

The GEOTHERMICA is supported by the European Union's HORIZON 2020 programme for research, technological development and demonstration under grant agreement No 731117

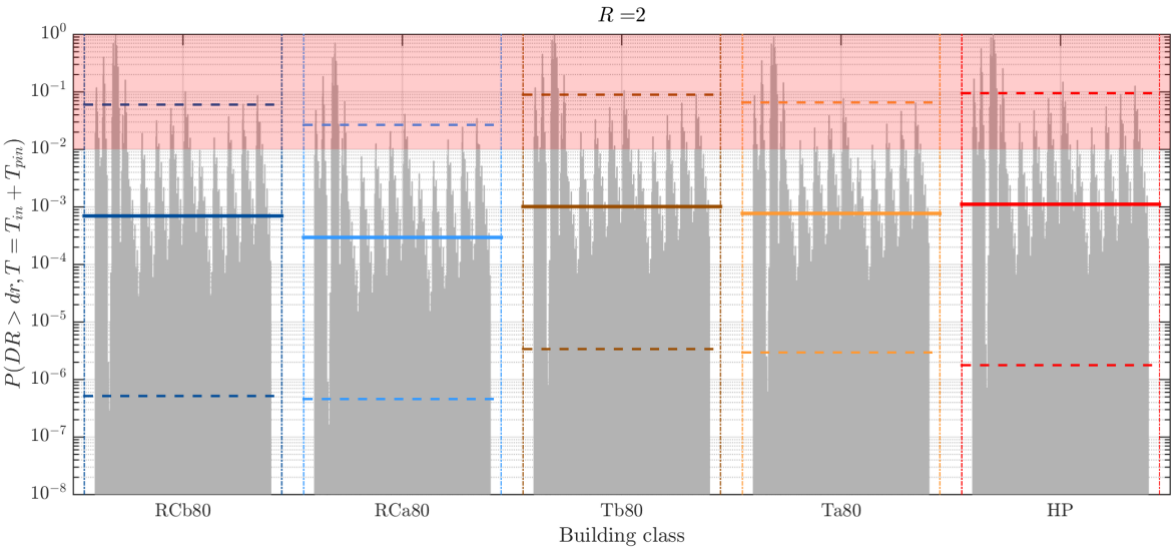

Figure 12 Marginal DR for the final model for 2 km distance, subject to change for different injection volumes. The solid horizontal lines represent the median values of the vertical gray lines. The dashed horizontal lines represent the 10 and 90% epistemic quantiles.

3 Online updating strategies for hazard and risk time evolution

At the present time, only model SM1 and SM2 are available. Complex 3D geomechanical models are under development, and a forward and inverse Uncertainty Quantification framework can be formulated only after the completion of WP3. In addition, the full inversion problem for SM2 is still under development; therefore, here we focus on the updating strategy for model SM1. In this section, we discuss only the updating of the rate model (i.e., only of $[a_{fb}, b, \tau]$), while the updating strategies for the coefficient of the GMPEs are not discussed (this will be part of future deliverables).

The real time updating strategy uses the full Non-Homogeneous Poisson process. In particular, we implement a classical Bayesian inverse framework (Broccardo et al. 2017), which allows a coherent classification and quantification of the epistemic and aleatory sources of uncertainty. Following SM1, we use the values reported in Table 1 to transform the hyper parameters into random variables. A major advantage of the Bayesian approach is that it enables uncertainties and expert judgments about the model's parameters to be encoded into a joint prior distribution. In this case, we include expert knowledge to determine the bounds of the parameters range. Once the project is started and physical information becomes available, the Bayesian framework allows the computation of the posterior distribution for the model's parameters, the formulation of predictive models and a robust forecasting strategy. The inference strategy for the empirical model proposed in this project, together with the predictive model for the number and magnitude of fluid-induced events are reported in detail in Broccardo et al. 2017. At the current time, we also integrated the hazard and risk computation but not the updates of the ground motion prediction equations. Figure 13 shows the joint prior distribution and the joint posterior after data are available for a blind synthetic dataset simulated with the model SM2. The correlation between the different parameters is zero because the minimum cut off magnitude is (for this example) set to zero. Figure 14 shows an iso-risk contour plot together with the posterior distribution. This plot, the first of this kind, shows both the "safe" and "risky" domain (after the full Hazard-Risk computation) and the epistemic uncertainty evolution around the parameters a_{fb} and b. Finally, Figure 15 shows the online evolution on IR together with the epistemic uncertainty reduction on its value.

The GEOTHERMICA is supported by the European Union's HORIZON 2020 programme for research, technological development and demonstration under grant agreement No 731117

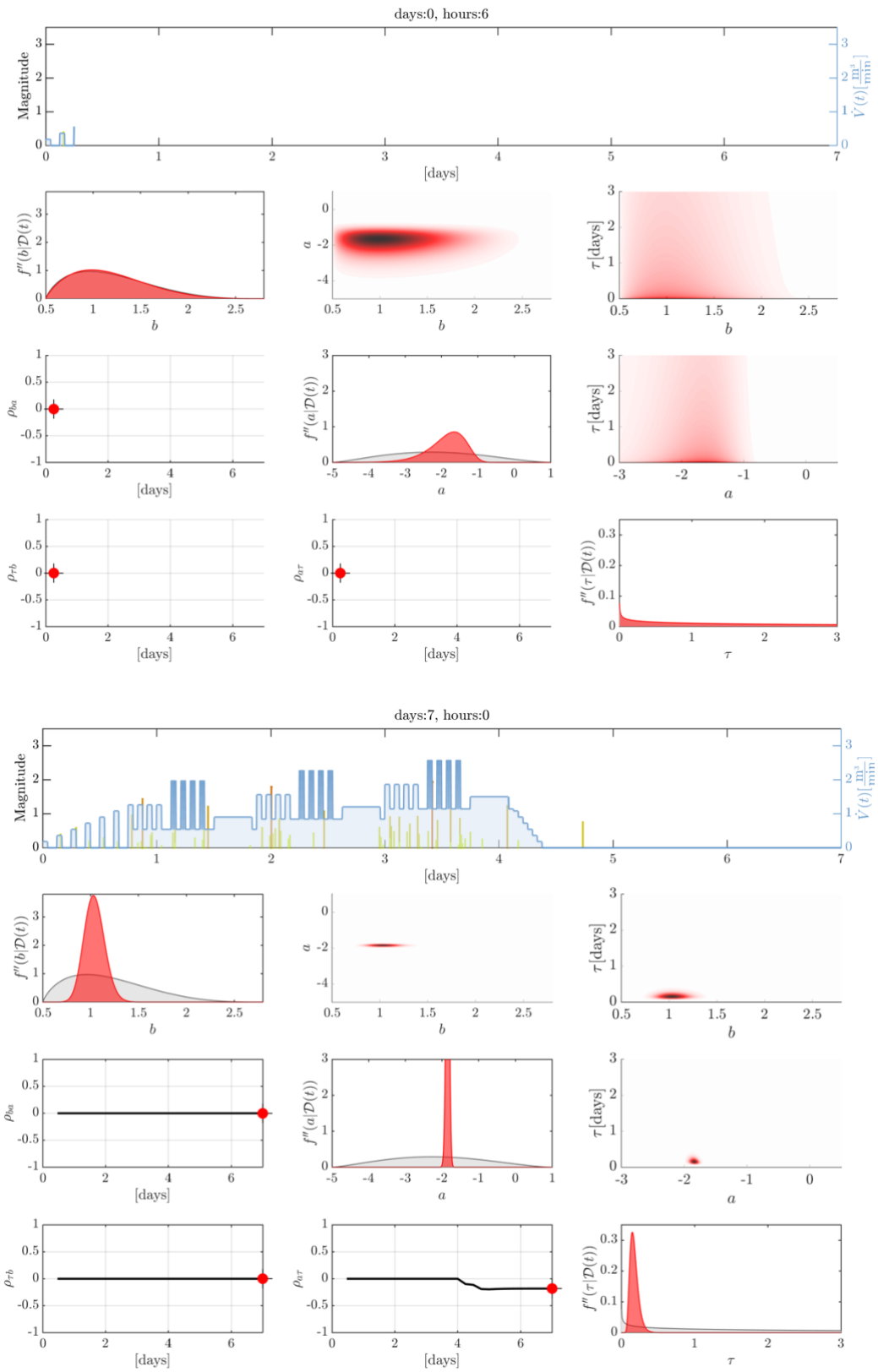

Figure 13 Synthetic data set. Marginal model parameter distributions: grey represents prior distributions, red represents posterior distribution, and lines correlation coefficient between the model parameters. First block, first updates; Second block, last updates.

The GEOTHERMICA is supported by the European Union's HORIZON 2020 programme for research, technological development and demonstration under grant agreement No 731117

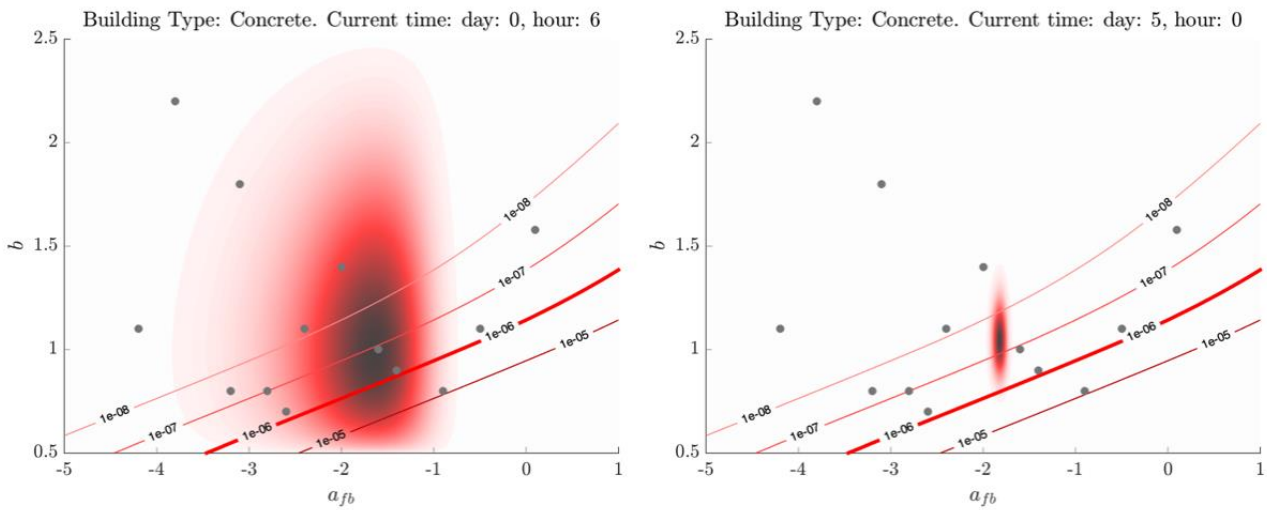

Figure 14 Synthetic data set for a virtual concrete building. Iso-risk curve and posterior distribution, left panel first updates, right panel last updates

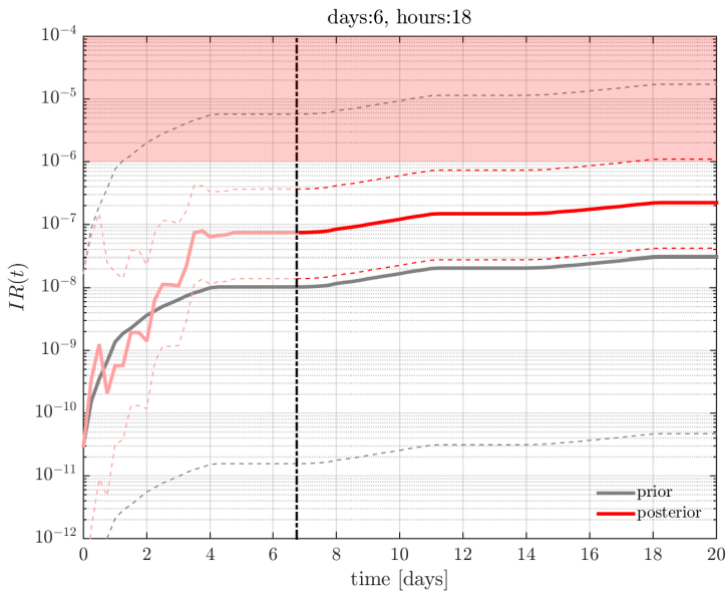

Figure 15 Risk updates and epistemic uncertainty reduction after 5 days of the updates. Solid line mean risk, dashed lines 5-95% quantiles. Grey lines computations based on prior uncertainties; red lines computations based on 5 days posterior. Observe the large uncertainty reduction.

Conclusions

In this deliverable, we presented the first version of the hazard and risk framework for fluid-induced seismicity to be tested in the Hengill region in Iceland. Currently, we defined the full a-priori hazard and risk assessment framework, which is used as “prior” information for the updating scheme. Next, we introduced a Bayesian framework to update the source models and preformed a “blind” test on a synthetic data set. The future work will focus on designing a full Bayesian inversion analysis for a 3D Geomechanical model, which is under development in WP3, together with the updating of the GMPEs coefficients and weights. Next, we will test the full framework with real data. From these analyses, we will finally design a probabilistic classification scheme to discriminate induced events from natural events.

The GEOTHERMICA is supported by the European Union’s HORIZON 2020 programme for research, technological development and demonstration under grant agreement No 731117

References

Ambraseys, N. N., Douglas, J., Sarma, S. K., and Smit, P. M. Equations for the estimation of strong ground motions from shallow crustal earthquakes using data from Europe and the Middle East: horizontal peak ground acceleration and spectral acceleration. Bulletin of earthquake engineering, 3(1), 1-53, doi: 10.1007/s10518-005-0183-0, 2005.

Akkar, S., and Bommer, J. J. Empirical equations for the prediction of PGA, PGV, and spectral accelerations in Europe, the Mediterranean region, and the Middle East. Seismological Research Letters, 81(2), 195-206, doi: 10.1785/gssrl.81.2.195, 2010.

Bessason, B., & Bjarnason, J. Ö. Seismic vulnerability of low-rise residential buildings based on damage data from three earthquakes (Mw6. 5, 6.5 and 6.3). Engineering Structures, 111, 64-79, doi: 10.1016/j.engstruct.2015.12.008, 2016.

Bommer, J. J., Crowley, H., & Pinho, R. A risk-mitigation approach to the management of induced seismicity. Journal of Seismology, 19(2), 623-646, doi 10.1007/s10950-015-9514-z, 2015.

Broccardo, M., Mignan, A., Grigoli, F., Karvounis, D., Rinaldi, A. P., Danciu, L., Hofmann, H., Milkereit, C., Dahm, T., Zimmermann, G., Hjörleifsdóttir, V., and Wiemer, S.: Induced seismicity risk analysis of the hydraulic stimulation of a geothermal well on Geldinganes, Iceland, Nat. Hazards Earth Syst. Sci. Discuss., https://doi.org/10.5194/nhess-2019-331, in review, 2019.

Broccardo, M., Mignan, A., Wiemer, S., Stojadinovic, B., and Giardini, D. Hierarchical Bayesian Modeling of Fluid-Induced Seismicity. Geophysical Research Letters, 44(22), 11-357, doi: 10.1002/2017GL075251, 2017a.

Broccardo, M., Danciu, L., Stojadinovic, B., and Wiemer, S. Individual and societal risk metrics as parts of a risk governance framework for induced seismicity. In 16th World Conference on Earthquake Engineering (WCEE16), 2017b.

Cauzzi, C., & Faccioli, E. Broadband (0.05 to 20 s) prediction of displacement response spectra based on worldwide digital records. Journal of Seismology, 12(4), 453. doi: 10.1007/s10950-008-9098-y, 2008.

Cornell, C. A. Engineering seismic risk analysis. Bulletin of the seismological society of America, 58(5), 1583-1606, 1968.

Danciu, L., and Tselentis, G. A. Engineering ground-motion parameters attenuation relationships for Greece. Bulletin of the Seismological Society of America, 97(1B), 162-183, doi: 10.1785/0120050087, 2007.

Dinske, C., and Shapiro, S. A. Seismotectonic state of reservoirs inferred from magnitude distributions of fluid-induced seismicity. Journal of seismology, 17(1), 13-25, doi: 10.1007/s10950-012-9292-9, 2013.

Faccioli, E., and Cauzzi, C. Macroseismic intensities for seismic scenarios estimated from instrumentally based correlations. In Proc. First European Conference on Earthquake Engineering and Seismology, paper (No. 569), 2006.

Faenza, L., and Michelini, A. Regression analysis of MCS intensity and ground motion parameters in Italy and its application in ShakeMap. Geophysical Journal International, 180(3), 1138-1152, doi:10.1111/j.1365-246X.2009.04467.x, 2010.

Grigoli, F., Cesca, S., Priolo, E., Rinaldi, A. P., Clinton, J. F., Stabile, T. A., ... & Dahm, T. Current challenges in monitoring, discrimination, and management of induced seismicity related to underground industrial activities: A European perspective. Reviews of Geophysics, 55(2), 310-340. doi: 10.1002/2016RG000542, 2017.

The GEOTHERMICA is supported by the European Union's HORIZON 2020 programme for research, technological development and demonstration under grant agreement No 731117

Grünthal, G. European macroseismic scale 1998. European Seismological Commission (ESC), 1998.

Gülkan, P., and Kalkan, E. Attenuation modeling of recent earthquakes in Turkey. Journal of Seismology, 6(3), 397-409, doi: 10.1023/A:1020087426440, 2002.

Karvounis, D. C., Gischig, V. S., and Wiemer, S. Towards a real-time forecast of induced seismicity for enhanced geothermal systems. In Shale Energy Engineering 2014: Technical Challenges, Environmental Issues, and Public Policy (pp. 246-255), doi: 10.1061/9780784413654.026, 2014.

Karvounis, D. C., and Jenny, P. Adaptive Hierarchical Fracture Model for Enhanced Geothermal Systems. Multiscale Modeling & Simulation, 14(1), 207–231, doi: 10.1137/140983987, 2016.

Kowsari, M., Halldorsson, B., Hrafnkelsson, B., Snæbjörnsson, J. Þ., and Jónsson, S. Calibration of ground motion models to Icelandic peak ground acceleration data using Bayesian Markov Chain Monte Carlo simulation. Bulletin of Earthquake Engineering, 17(6), 2841-2870, doi: 10.1007/s10518-019-00569-5, 2019.

Lagomarsino, S. and Giovinazzi, S. Bull Earthquake Engineering, 4: 415, doi: 10.1007/s10518-006-9024-z, 2006.

Lee, K.K., Ellsworth, W.L., Giardini, D., Townend, J., Shemin Ge, Shimamoto, T., Yeo, In-W., Kang, Tae-S., Rhie, J., Sheen, D.-H., Chang, C., Wool, J.-U., and C. Langenbruch. Managing injection-induced seismic risks. Science 364 (6442), 730-732, doi: 10.1126/science.aax1878, 2019.

Mignan, A., Landtwing, D., Kästli, P., Mena, B., and Wiemer, S. Induced seismicity risk analysis of the 2006 Basel, Switzerland, Enhanced Geothermal System project: Influence of uncertainties on risk mitigation. Geothermics, 53, 133-146, doi: 10.1016/j.geothermics.2014.05.007, 2015.

Mignan, A.: Static behaviour of induced seismicity, Nonlin. Processes Geophys., 23, 107–113, doi: 10.5194/npg-23-107-2016, 2016.

Mignan, A., Broccardo, M., Wiemer, S., and Giardini, D. Induced seismicity closed-form traffic light system for actuarial decision-making during deep fluid injections. Scientific reports, 7(1), 13607, doi: 10.1038/s41598-017-13585-9, 2017.

Rupakhety, R., and Sigbjörnsson, R. Ground-motion prediction equations (GMPEs) for inelastic displacement and ductility demands of constant-strength SDOF systems. Bulletin of Earthquake Engineering, 7(3), 661-679, doi: 10.1007/s10518-009-9117-6, 2009.

van der Elst, N. J., M. T. Page, D. A. Weiser, T. H. W. Goebel and S. M. Hosseini. Induced earthquake magnitudes are as large as (statistically) expected, J. Geophys. Res. Solid Earth, 121, 4575-4590, doi: 10.1002/2016JB012818, 2016.

Zhao, J.X., Zhang, J., Asano, A., Ohno, Y., Oouchi, T., Takahashi, T., Ogawa, H., Irikura, K., Thio, H.K., Somerville, P.G. and Fukushima, Y. Attenuation relations of strong ground motion in Japan using site classification based on predominant period. Bulletin of the Seismological Society of America, 96(3), pp.898-913, doi: 10.1785/0120050122, 2006.

The GEOTHERMICA is supported by the European Union's HORIZON 2020 programme for research, technological development and demonstration under grant agreement No 731117